

First-principles calculations of high pressure and temperature properties of Fe_7C_3

Li-Li Fan(范莉莉), Xun Liu(刘勋), Chang Gao(高畅), Zhong-Li Liu(刘中利), Yan-Li Li(李艳丽), and Hai-Jun Huang(黄海军)

Citation: Chin. Phys. B, 2023, 32 (**7**): 079101. DOI: 10.1088/1674-1056/acb915
Journal homepage: http://cpb.iphy.ac.cn; http://iopscience.iop.org/cpb

What follows is a list of articles you may be interested in

The structure and elasticity of phase B silicates under high pressure by first principles simulation

Lei Liu(刘雷), Li Yi(易丽), Hong Liu(刘红), Ying Li(李营), Chun-Qiang Zhuang(庄春强), Long-Xing Yang(杨龙星), Gui-Ping Liu(刘桂平)

Chin. Phys. B, 2018, 27 (**4**): 047402. DOI: 10.1088/1674-1056/27/4/047402

Elastic properties of $CaCO_3$ high pressure phases from first principles

Dan Huang(黄丹), Hong Liu(刘红), Ming-Qiang Hou(侯明强), Meng-Yu Xie(谢梦雨), Ya-Fei Lu(鹿亚飞), Lei Liu(刘雷), Li Yi(易丽), Yue-Ju Cui(崔月菊), Ying Li(李营), Li-Wei Deng(邓力维), Jian-Guo Du(杜建国)

Chin. Phys. B, 2017, 26 (**8**): 089101. DOI: 10.1088/1674-1056/26/8/089101

Mechanical and thermodynamic properties of cubic YH_2 under high pressure：Prediction from first-principles study

Li Zhen-Li (李贞丽), Cheng Xin-Lu (程新路)

Chin. Phys. B, 2014, 23 (**4**): 046201. DOI: 10.1088/1674-1056/23/4/046201

First-principles calculations of high pressure and temperature properties of Fe_7C_3

Li-Li Fan(范莉莉)[1], Xun Liu(刘勋)[1], Chang Gao(高畅)[1], Zhong-Li Liu(刘中利)[2], Yan-Li Li(李艳丽)[1], and Hai-Jun Huang(黄海军)[1,†]

[1] *School of Science, Wuhan University of Technology, Wuhan* 430070, *China*
[2] *School of Materials Science and Engineering, Harbin Institute of Technology, Harbin* 150001, *China*

(Received 14 September 2022; revised manuscript received 25 December 2022; accepted manuscript online 6 February 2023)

Eckstrom–adcock iron carbide (Fe_7C_3) is considered to be the main constituent of the Earth's inner core due to its low shear wave velocity. However, the crystal structure of Fe_7C_3 remains controversial and its thermoelastic properties are not well constrained at high temperature and pressure. Based on the first-principles simulation method, we calculate the relative phase stability, equation of state, and sound velocity of Fe_7C_3 under core condition. The results indicate that the orthorhombic phase of Fe_7C_3 is stable under the core condition. While Fe_7C_3 does reproduce the low shear wave velocity and high Poisson's ratio of the inner core, its compressional wave velocity and density are 12% higher and 6% lower than those observed in seismic data, respectively. Therefore, we argue that carbon alone cannot completely explain the thermal properties of the inner core and the inclusion of other light elements may be required.

Keywords: iron carbide, phase stability, thermoelastic properties, sound velocities, inner core

PACS: 91.60.Fe **DOI:** 10.1088/1674-1056/acb915

1. Introduction

As is well known, the Earth's core is composed of Fe–Ni alloy with a small quantity of light elements. Based on geochemical and meteorological studies, light elements most likely originate from carbon (C), hydrogen (H), oxygen (O), sulfur (S), and silicon (Si).[1] Until now, the light elemental composition of the Earth's core has been poorly understood. Among these light elements, C has been suggested as a major light elemental component of the Earth's core, as C is enriched in the solar system [2] and has a high affinity for liquid iron under core–mantle differentiation conditions.[3] In addition, the shear wave velocity and Poisson's ratio of Fe_7C_3 are similar to those of the inner core[4,5] and Fe_7C_3 melting experiments indicate that C might be a potential light element in the inner core.[6]

However, whether Fe_7C_3 is stable under core condition and the nature of its relatively stable structure remain unclear. Based on previous experimental results, two potential stable structures can be reasonably hypothesized at high temperature and pressure: hexagonal structure (space group $P6_3mc$; h-Fe_7C_3) and orthorhombic structure (space group *Pnma*, *Pmn*21*mc*, or *Pbca*; o-Fe_7C_3).[5,7–9] Nakajima *et al.* found that h-Fe_7C_3 is stable up to 71.5 GPa and 1973 K by using *in situ* x-ray diffraction.[10] Prescher *et al.* suggested that o-Fe_7C_3 is the more stable phase up to 205 GPa and 3700 K by using single-crystal and powder x-ray diffraction.[5] Theoretical calculations have been similarly inconclusive and often inconsistent. Fang *et al.* found that the o-Fe_7C_3 phase is more stable than h-Fe_7C_3 under ambient conditions.[11] Raza *et al.* found that o-Fe_7C_3 (space group *Pbca*) is stable below 100 GPa, while h-Fe_7C_3 becomes more stable above 150 GPa and requires higher temperatures for stability.[12]

The thermal equation of state (EOS) of Fe_7C_3 was measured experimentally only at low pressures and temperatures. Litasov *et al.*[13] and Nakajima *et al.*[10] measured the EOS below 30 GPa; however, their results deviate widely when extrapolated to the high temperature and pressure conditions of the inner core. Chen and Zhang acquired compressional (V_P) and shear wave velocity (V_S) data for Fe_7C_3 up to 154 GPa at 300 K by using x-ray diffraction.[4] Subsequently, Prescher *et al.* investigated the V_P and V_S for Fe_7C_3 up to 158 GPa and 300 K by using the same method.[5] However, these sound velocity measurements of Fe_7C_3 exhibited large discrepancies.[4,5] Therefore, it is necessary to investigate the crystal structure and thermoelastic properties of Fe_7C_3 under core condition to ascertain the amount of carbon present in the inner core.

Here, using first-principles calculations, we estimate the free energy, EOS, and sound velocity of Fe_7C_3. The EOS and sound velocity data for Fe_7C_3 are calculated at 0 K–5000 K, which is close to the inner core boundary temperature obtained by phonon spectrum calculations. We also use our findings to discuss whether carbon is the main light element present in the inner core.

[†]Corresponding author. E-mail: hjhuang@whut.edu.cn

© 2023 Chinese Physical Society and IOP Publishing Ltd

2. Methods

All calculations were performed by using the Vienna *ab initio* simulation package (VASP) based on density functional theory (DFT).[14] The conjugate gradient (CG) algorithm was adopted for the geometric optimization of the crystal structures. Exchange–correlation interactions were considered as the Perdew–Burke–Ernzerhof (PBE) parametrization of the gradient approximation (GGA).[15] The electron–ion interactions were represented by projected augmented-wave (PAW) pseudopotentials.[16,17] The simulation cell contained 40 atoms for o-Fe_7C_3. Prior to formal calculation, we calculated the free energy values of 40 and 20 atoms for h-Fe_7C_3 at some pressure points, obtaining highly similar results. To balance the computational efficiency and precision, we selected 20 atoms for h-Fe_7C_3 calculation at all pressure points. The cutoff energy was 500 eV. The Monkhorst–Pack mesh was $6\times4\times7$ for o-Fe_7C_3 and $6\times6\times9$ for h-Fe_7C_3.[18] The phonon spectra and free energy of o-Fe_7C_3 and h-Fe_7C_3 were calculated and analyzed by using the Phonopy[19] and Phasego programs.[20] The phonon spectra and Helmholtz free energy were calculated up to 360 GPa in the quasi-harmonic approximation (QHA). During the thermodynamic simulations, we constructed $1\times1\times2$ and $1\times2\times2$ supercells for o- and h-Fe_7C_3, and set denser k-point meshes to $7\times5\times3$ and $6\times6\times9$ grids, respectively.[21–23]

Previous studies have reported that Fe_7C_3 undergoes a magnetic transition from a ferromagnetic (FM) to nonmagnetic (NM) phase at high pressure.[5] Therefore, we performed spin-limited and unlimited calculations to investigate the effect of spin on the EOS.

The elastic constant of Fe_7C_3 was estimated by using the stress-strain method.[24] Force constant was calculated in real space by using density functional perturbation theory. The bulk modulus and shear modulus were calculated from the elastic tensor by using the Voight–Hill–Reuss method.[24,25] Sound velocities were obtained from the following formulas:

$$V_{\mathrm{P}}=\sqrt{(B+4G)/\rho}, \tag{1}$$

$$V_{\mathrm{S}}=\sqrt{G/\rho}, \tag{2}$$

where V_{P} is the compressional wave velocity, V_{S} is the shear wave velocity, B is the bulk modulus, G is the shear modulus, and ρ is the density. Considering the symmetry of Fe_7C_3, B and G can be expressed as

$$B=\frac{C_{11}+C_{22}+C_{33}+2(C_{12}+C_{13}+C_{23})}{9}, \tag{3}$$

$$G=\frac{C_{11}+C_{22}+C_{33}-(C_{12}+C_{13}+C_{23})+3(C_{44}+C_{55}+C_{66})}{15}, \tag{4}$$

where C_x ($x=11$, 22, 33, 44, 55, 66, 12, 13, or 23) values are all elastic constants.

3. Results

3.1. Relative stabilities of o- and h-phase Fe_7C_3

To determine which structure is stable, we calculate the Gibbs free energy values of o-Fe_7C_3 and h-Fe_7C_3 at high pressure and temperature (Fig. 1). The difference in Gibbs free energy in o-Fe_7C_3 and h-Fe_7C_3 is a function of temperature. At 120 GPa, the free energy value of o-Fe_7C_3 is 14 meV/atom at 0 K and 72 meV/atom at 4000 K, less than the counterparts of h-Fe_7C_3. At 360 GPa, the free energy of o-Fe_7C_3 is 17 meV/atom more than that of h-Fe_7C_3 at 0 K, but is 29 meV/atom less than that of h-Fe_7C_3 at 4000 K. Thus, the free energy of o-Fe_7C_3 is less than that of h-Fe_7C_3 at high temperatures. In this study, the energy value of self-consistent optimization convergence is set to 10^{-5} eV, which is much smaller than the difference between the free energy values. Therefore, o-Fe_7C_3 appears to be more stable than h-Fe_7C_3 under inner core condition. Hereafter, we investigate the thermal properties of o-Fe_7C_3 (instead of h-Fe_7C_3[26,27]) at high temperature and high pressure.

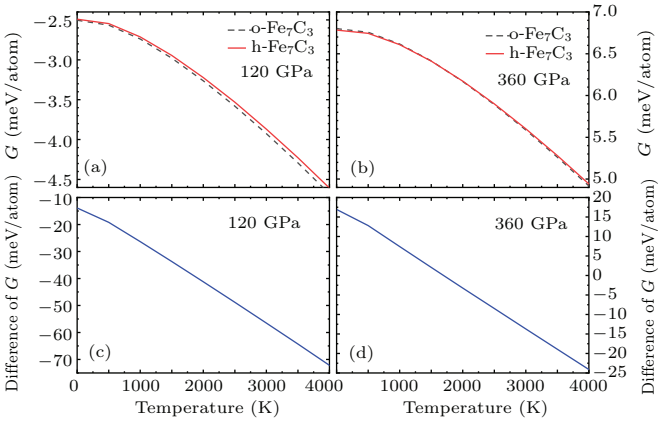


Fig. 1. Free energy values of o-Fe_7C_3 and h-Fe_7C_3 under simultaneous action of high pressure and high temperature, showing temperature-dependent (a) Gibbs free energy at 120 GPa, (b) Gibbs free energy at 360 GPa, and (c) at 120 GPa temperature-dependent difference in Gibbs free energy between o-Fe_7C_3 and h-Fe_7C_3; (d) at 360 GPa temperature-dependent difference in Gibbs free energy between o-Fe_7C_3 and h-Fe_7C_3.

3.2. Thermal EOS of o-Fe_7C_3

The Fe_7C_3 is magnetic at low pressures and undergoes magnetic collapse at high pressures.[5] Consequently, we calculate the EOSs for o-Fe_7C_3 with and without spin at 0 K. Figure 2 shows a comparison between the results of this study and previous results from the static compression method at room temperature[5,10,28,29] and *ab initio* simulations,[13,26,30] whose detailed comparisons can be found in supplementary Table 3. Below 50 GPa, the EOSs with spin consideration are consistent with static measurements at 300 K[5,10,28,29] and *ab initio* simulations,[13,30] all of which are higher than the simulated results without spin consideration.[13,26] With the increase of pressure, the EOSs with spin restrictions began to converge with the EOSs without spin restrictions due to demagnetization at $\sim$ 70 GPa–100 GPa, implying the presence of a spin

phase transition. The transition pressure is consistent with that observed by using the static compression method.[5] The discontinuity in the EOS of Fe_7C_3 near 53 GPa (or 70 GPa) is presumably attributed to a transition from a high- to low-spin state.[5,29] At 300 K, the extrapolations of the experimental measurements are different from each other considerably at inner core pressures (Fig. 2), and the results obtained herein accord with the Prescher *et al.*'s results.[5] The differences from previous experimental results may be related to their samples, some of which were based on powder x-ray diffraction data,[29] whereas the structure reported by Prescher *et al.* was based on single-crystal x-ray diffraction data.[5] The pressure and density data of the non-magnetic phase fit the third-order Birch–Murnaghan (BM) equation[31]

$$P = \frac{3}{2}B_0\left[\left(\frac{\rho}{\rho_0}\right)^{7/3} - \left(\frac{\rho}{\rho_0}\right)^{5/3}\right] \times \left\{1 + \frac{3}{2}\left(B_0' - 4\right)\left[\left(\frac{\rho}{\rho_0}\right)^{2/3} - 1\right]\right\}, \quad (5)$$

where P is the pressure, ρ_0 is the initial density, B_0 is the bulk modulus, and B_0' is the pressure derivative. Thus, the bulk modulus $B_0 = 322 \pm 1$ GPa and its pressure derivative $B_0' = 4.38 \pm 0.02$ can be obtained.

Figure 3 shows the linear compression ratio of Fe_7C_3 at high pressure. The largest compression ratio is along the a axis, while the smallest one is along the c axis, indicating that Fe_7C_3 turns anisotropic under compression. The compressibility along the a axis is greater than that along the b axis and the c axis because the Fe–Fe bond is along the a axis, which is stronger and tighter than the Fe–C bond along the b axis and c axis. Although the compression ratios are different from those observed in static experiments, their variation trends along all three axes are consistent with previous experimental results.[28]

To ascertain the carbon content of the inner core, we calculate the thermal EOS of o-Fe_7C_3 at high temperature and pressure by using QHA[22] (Fig. 4).

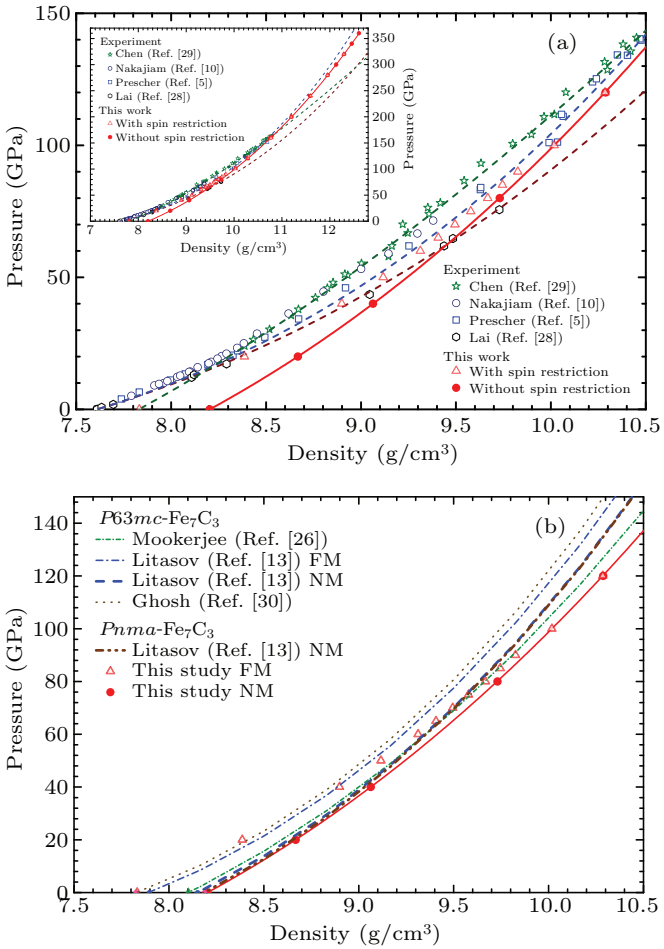


Fig. 2. (a) Static isotherms of Fe_7C_3 obtained in this study and cited from (a) other static experimental studies and (b) other theoretical studies, where solid and dashed lines denote the third-order Birch–Murnaghan fittings to the simulation results and experimental results.

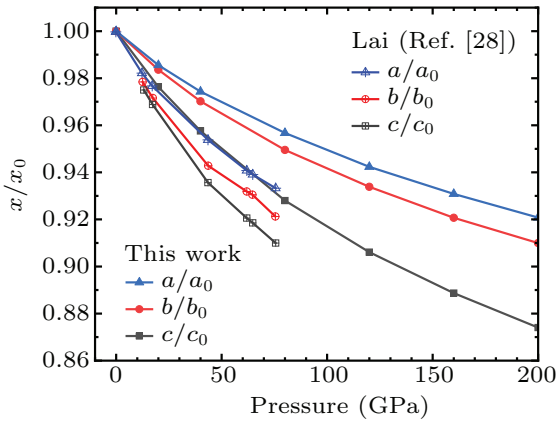


Fig. 3. Compression ratios varying with pressure in different directions.

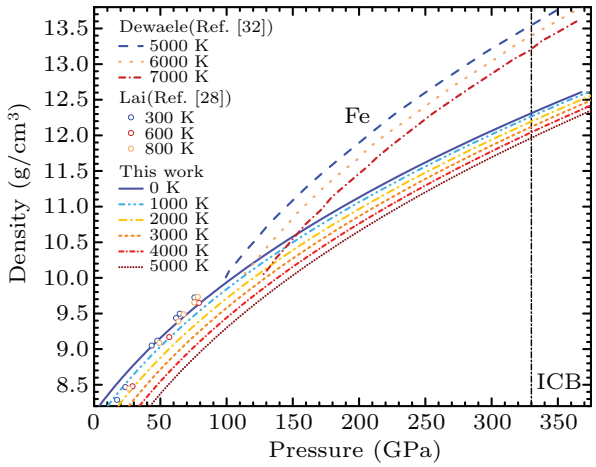


Fig. 4. Equation of states of Fe_7C_3 at specific temperatures from 0 GPa to 360 GPa (dashed lines indicate Fe isotherms).

In general, the results obtained herein are consistent with the experimental measurements of Lai.[28] In addition, we calculate the EOSs for h-Fe_7C_3 in this study, but they almost coincide with those obtained for o-Fe_7C_3 at high temperature and pressure. The data for pure Fe are also shown here for comparison.[32] At inner core pressures, the density of Fe_7C_3 is 9.47% lower than that of pure Fe at a temperature of 5000 K.

3.3. Sound velocities

To ascertain the carbon content of the inner core, it is necessary to determine the elastic properties of Fe_7C_3 at high temperatures and pressures. However, there are clear differences among the experimental measurements of sound velocities in Fe_7C_3 at high pressures (Fig. 5), even at room temperature. In this study, the sound velocity of Fe_7C_3 at 0 K is calculated by using the method described in Section 2. Because we are more interested in the sound velocity of Fe_7C_3 at core pressure, we only calculate the sound velocity for Fe_7C_3 without spin restriction (Fig. 5).

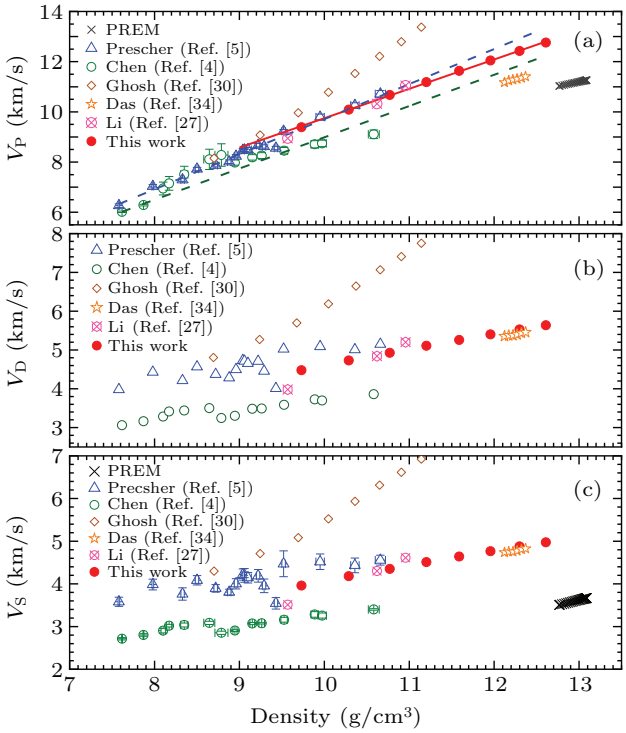


Fig. 5. Sound velocities of Fe_7C_3 obtained in this and previous studies, where Xs are cited from the preliminary reference Earth model [PREM],[33] showing density-dependent (a) compressional waves, (b) Debye velocities, and (c) shear wave velocities.

The calculated V_P of Fe_7C_3 increases linearly with density, complying with Birch's law: $V_P = -1.72\,(\pm 0.12) + 1.15(\pm 0.01)\rho$. At 0 K, the calculated V_S is also linearly related to the density, $V_S = 0.66\,(\pm 0.05) + 0.34\,(\pm 0.00)\,\rho$. The Debye velocity ($V_D$) of Fe_7C_3 can be calculated from the following formula:

$$\frac{3}{V_D^3} = \frac{1}{V_P^3} + \frac{2}{V_S^3}. \tag{6}$$

The calculated V_P, V_D, and V_S at 0 K are broadly consistent with the experimental results at 300 K obtained by Prescher *et al.*,[5] and higher than those obtained by Chen and Zhang,[4] particularly at high pressures. Figure 5 also shows the ab initio values.[27,30] The results obtained herein are similar to those obtained by Li *et al.*[27] and Das *et al.*,[34] but they are all less than those calculated by Ghosh *et al.*[30] Ghosh *et al.* also suggested that this deviation might be attributed to the nonlinear mixing of phonon modes.[30]

4. Geophysical implications for inner core composition

According to the results of this study, the effect of temperature on the sound velocity of Fe_7C_3 is unknown. Our previous experimental results for Fe and Fe–Si alloys suggest that Birch's law holds true at high temperatures and pressures.[35] Assuming that the V_P of Fe_7C_3 follows Birch's law at high temperatures, we obtain the V_P of Fe_7C_3 after determining its density at inner core. The bulk wave velocity (V_B) of Fe_7C_3 at high temperatures is calculated according to its EOS given as follows:

$$V_B = \sqrt{\frac{K_S}{\rho}}, \tag{7}$$

$$K_S = (1 + \alpha\gamma T)\,K_T, \tag{8}$$

where K_S and K_T are the bulk modulus along the isentrope and the isotherm, respectively; ρ is the density; α is the thermal expansion coefficient; and γ is the Grüneisen parameter. The value of α, γ, and K_T eachare obtained from the phonon spectrum, and V_S at high temperatures is obtained from the following formula:

$$V_S^2 = \frac{3\left(V_P^2 - V_B^2\right)}{4}, \tag{9}$$

and Poisson's ratio is calculated from the following equation:

$$\sigma = \frac{V_P^2 - 2V_S^2}{2(V_P^2 - V_S^2)}. \tag{10}$$

The temperature profile of the inner core is calculated by using $T = T_{ICB}(\rho/\rho_{ICB})^{\gamma}$. The preferred value of T_{ICB} and γ are 5400 K and 1.5.[1] However, in this study, we only calculate the data for $T_{ICB} = 5000$ K, as QHA often introduces large errors when the temperature is sufficiently high or close to the melting temperature of Fe_7C_3.[36] The reliability of QHA at high temperatures has been discussed previously.[37] Figure 6 shows the calculated value of ρ, V_P, V_S, and σ of Fe_7C_3 and the comparison with the values of preliminary reference Earth model (PREM).[33] Except for the density, the simulated V_P, V_S, and σ of Fe_7C_3 obtained in this study deviated from those obtained by Das *et al.*[34]

The density of Fe and Fe_7C_3 are about 5.87% higher and 6.34% lower than the PREM values respectively in the whole range of Earth's inner core pressure. The Fe_7C_3 content of 44.71 wt% can explain the density deficit of the inner core (Fig. 6(a)) if carbon is the only light element in the core and is present as Fe_7C_3. Under the inner core condition, the value of V_S and σ of Fe_7C_3 are very close to the PREM values compared with those of Fe (Fig. 6(c)). The V_P of Fe_7C_3 is

slightly higher than that of Fe, and both are much larger than the PREM values. Thus, carbon might be ruled out as the major light element in the Earth's inner core, which is consistent with findings of Fe–C phase,[38] Fe–C solid solution,[39] and geochemical[40] investigations. By analyzing the Fe–C phase diagram at high temperatures and pressures, Fei *et al.* suggested that the carbon content of the inner core is about 2.24%.[38] More recently, Huang *et al.* experimentally determined Fe–C solid solution densities up to core pressures, and concluded that interstitial carbon can lower the density of iron and be present in the inner core.[39] Using geochemical methods, McDonough concluded that the carbon content of the inner core is less than 0.2%.[40] Therefore, if carbon is present in the inner core, other light elements must also be present, which has inspired many studies of the Fe–C–Si ternary system. Pamato *et al.* proposed an Fe–C–Si model for the inner core composition based on the EOS of Fe–C–Si at high pressures and temperatures.[41] Das *et al.* found that doping a small quantity of Si impurities at carbon sites in Fe_7C_3 carbide phases can reduce the V_P and V_S, which are closer to the PREM data.[34] According to the V_P and V_S velocities of Fe and Fe-8.6Si, and combining the V_P and V_S results of Fe_7C_3 obtained by Chen and Zhang,[4] Huang *et al.*[35] suggested that the density and sound velocity for an Fe–C–Si inner core both match the PREM values. However, the V_P and V_S data obtained by Chen *et al.* are less than our calculated results and the *ab initio* values obtained by Li *et al.*,[27] as well as the experimental data obtained by Prescher *et al.*[5] Therefore, further experiments are required to investigate the V_P and V_S of Fe_7C_3, particularly at high temperatures.

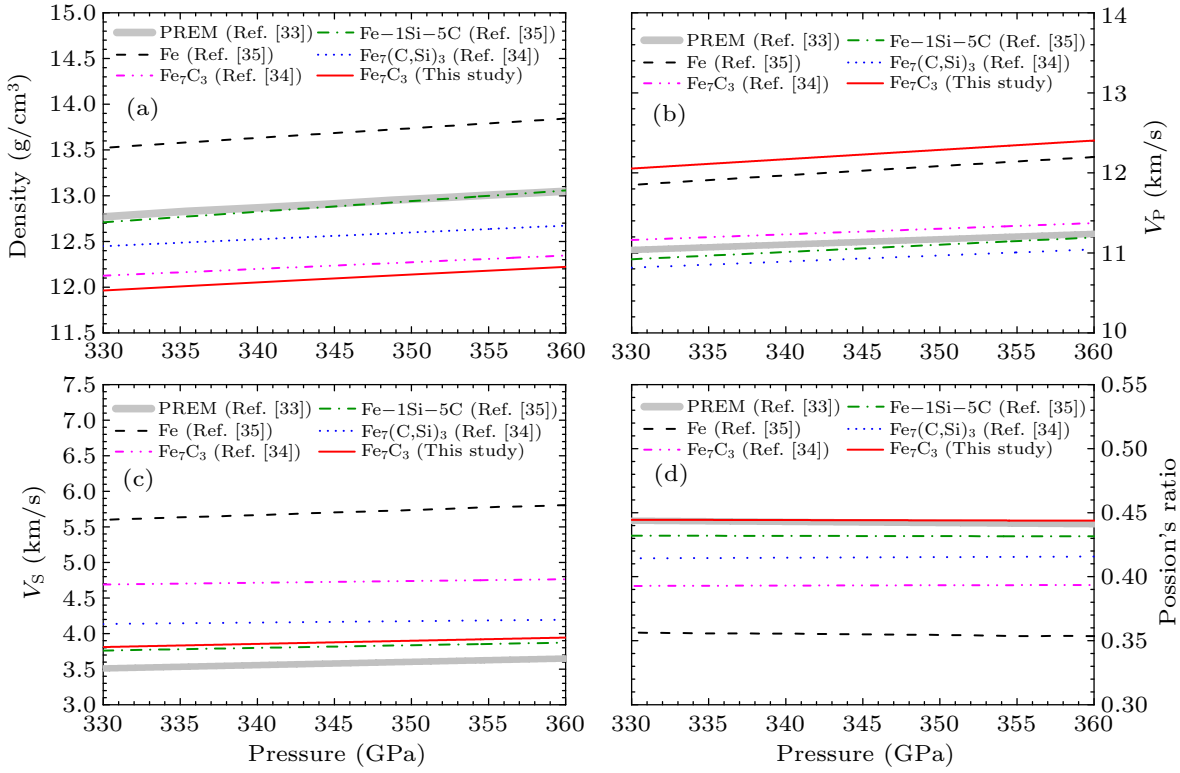


Fig. 6. (a) Pressure-dependent calculated densities of Fe (black line)[35] and Fe_7C_3 (red line), assuming a temperature of 5000 K, compared with the PREM[33] density profile. Fe_7C_3 (pink line) and $Fe_7(C,Si)_3$ (blue dotted line) are cited from Ref. [34]. Fe–1Si–5C (green dotted line) is cited from Ref. [35]. (b) Pressure-dependent compressional wave velocities and their comparisons. (c) Pressure-dependent shear wave celocities and their comparisons. (d) Pressure-dependent Poisson's ratios and their comparisons.

5. Conclusions

In the present study, the thermal equation of state (EOS) and sound velocities of Fe_7C_3 at high pressures are calculated by using first-principles methods. The simulated results are generally in agreement with the previous experimental results. Although the derived V_S and σ of Fe_7C_3 can reproduce the inner core values, the calculated V_P of Fe_7C_3 is higher than that of Fe and the inner core. Therefore, it is less likely for carbon to be present only as Fe_7C_3 in the Earth's core.

Acknowledgement

Project supported by the National Natural Science Foundation of China (Grant Nos. 41904085, 41874103, and 42274124).

References

[1] Hirose K, Labrosse S and Hernlund J 2013 *Annu. Rev. Earth Pl. Sci.* **41** 657
[2] Wood B J 1993 *Earth. Planet. Sci. Lett.* **117** 593
[3] Wood B J, Li J and Shahar A 2013 *Rev. Mineral. Geochem.* **75** 231

[4] Chen B, Li Z and Zhang D 2014 *Proc. Natl Acad. Sci. USA* **111** 17755
[5] Prescher C, Dubrovinsky L, Bykova E, Kupenko I, Glazyrin K, Kantor A, McCammon C, Mookherjee M, Nakajima Y and Miyajima N 2015 *Nat. Geosci.* **8** 220
[6] Liu J, Lin J F, Prakapenka V, Prescher C and Yoshino T 2016 *Geophys. Res. Lett.* **43** 12415
[7] Herbstein F H and Snyman J A 1964 *Inorg. Chem.* **3** 894
[8] Barinov V A, Tsurin V A and Surikov V T 2010 *Phys. Metals Metallogr.* **110** 474
[9] Bouchard J 1967 *Ann. Chim.* **2** 353
[10] Nakajima Y, Takahashi E, Sata N, Nishihara Y, Hirose K, Funakoshi K and Ohishi Y 2011 *Am. Mineral.* **96** 1158
[11] Fang C M, Van Huis M A and Zandbergen H W 2009 *Phys. Rev. B* **80** 224108
[12] Raza, Z, Shulumba N, Caffrey N M, Dubrovinsky L and Abrikosov I A 2015 *Phys. Rev. B* **91** 214112
[13] Litasov K D, Rashchenko S V, Shmakov A N, Palyanov Y N and Sokol A G 2015 *J. Alloys Compd.* **628** 102
[14] Kresse G and Furthmüller J 1996 *Phys. Rev. B* **54** 11169
[15] Perdew J P, Burke K and Ernzerhof M 1996 *Phys. Rev. Lett.* **77** 3865
[16] Blöchl P E 1994 *Phys. Rev. B* **50** 17953
[17] Kresse G and Joubert D 1999 *Phys. Rev. B* **59** 1758
[18] Monkhorst H J and Pack J D 1976 *Phys. Rev. B* **13** 5188
[19] Togo A and Tanaka I 2015 *Scr. Mater.* **108** 1
[20] Liu Z L 2015 *Comput. Phys. Commun.* **191** 150
[21] Wang V, Liang Y Y, Kawazeo Y and Geng W T 2018 arXiv: 1806.04285 [cond-mat.mes-hall]
[22] Wang V, Xu N, Liu J C, Tang G and Geng W T 2021 *Comput. Phys. Commun.* **267** 108033
[23] Hinuma Y, Pizzi G, Kumagai Y, Oba F and Tanaka I 2017 *Comput. Mater. Sci.* **128** 140
[24] Voigt W 1910 *Lehrbuch der Kristallphysik* (Leipzig: Teubner and Walsh J B) p. 12
[25] Simmons G and Wang H 1971 *Single Crystal Elastic Constants and Calculated Aggregate Progress: A Handbook* (Cambridge: MIT Press) p. 35
[26] Mookherjee M, Nakajima Y, Steinle-Neumann G, Glazyrin K, Wu X, Dubrovinsky L, McCammon C and Chumakov A 2011 *J. Geophys. Res. Solid Earth* **116** B04201
[27] Li Y, Vočadlo L, Brodholt J and Wood I G 2016 *J. Geophys. Res. Solid Earth* **121** 5828
[28] Lai X, Zhu F, Liu J, Zhang D, Hu Y, Finkelstein G J, Dera P and Chen B 2018 *Am. Mineral.* **103** 1568
[29] Chen B, Gao L, Lavina B, Dera P, Alp E, Zhao J and Li J 2012 *Geophys. Res. Lett.* **39** L18301
[30] Ghosh P S, Ali K, Vineet A, Voleti A and Arya A 2017 *J. Alloys Compd.* **726** 989
[31] Murnaghan F D 1944 *Proc. Natl Acad. Sci. USA* **30** 244
[32] Dewaele A, Loubeyre P, Occelli F, Mezouar M, Dorogokupets P I and Torrent M 2006 *Phys. Rev. Lett.* **97** 215504
[33] Dziewonski A M and Anderson D L 1981 *Phys. Earth. Planet. In.* **25** 297
[34] Das T, Chatterjee S, Ghosh S and Saha-Dasgupta T 2017 *Geophys. Res. Lett.* **44** 8776
[35] Huang H J, Fan L L, Liu X, Xu F, Wu Y, Yang G, Leng C W, Wang Q S, Weng J D, Wang X, Cai L C and Fei Y W 2022 *Nat. Commun.* **13** 1
[36] Liu J, Li J and Ikuta D 2016 *J. Geophys. Res. Solid Earth* **121** 1514
[37] Liu Z L, Cai L C, Chen X R, Wu Q and Jing F Q 2009 *J. Phys-Condens. Mat.* **21** 095408
[38] Fei Y, Murphy C, Shibazaki Y, Shahar A and Huang H 2016 *Geophys. Res. Lett.* **43** 6837
[39] Huang Y Q, Hou M Q, Gan B, Li X H, He D W, Jiang G, Zhang Y J and Liu Y 2022 *J. Geophys. Res. Solid Earth* **127** e2021JB023645
[40] McDonough W F 2003 *Treat. Geochem.* **2** 547
[41] Pamato M G, Li Y, Antonangeli D, Miozzi F, Morard G, Wood I G, Vočadlo L, Brodholt J P and Mezouar M 2020 *JJ. Geophys. Res. Solid Earth* **125** e2020JB020159